ACS Macro Letters

Letter

Cite This: ACS Macro Lett. 2019, 8, 1449−1455

pubs.acs.org/macroletters

Gelation Mechanism and Structural Dynamics of Chitosan Self-Healing Hydrogels by In Situ SAXS and Coherent X-ray Scattering

Yu-Jie Lin,[†] Wei-Tsung Chuang,[‡] and Shan-hui Hsu*,[†]

[†]Institute of Polymer Science and Engineering, National Taiwan University, No. 1, Sec. 4, Roosevelt Road, Taipei 10617, Taiwan, R.O.C.

[‡]National Synchrotron Radiation Research Center, Hsinchu 30076, Taiwan, R.O.C.

Supporting Information

ABSTRACT: Self-healing hydrogels with intrinsic self-healing ability, injectability, and biocompatibility have good potential in biomedical applications. The relevance between the self-healing ability and inner structure of hydrogels, however, has rarely been examined. The design criteria of self-healing hydrogels remain to be established. In this study, we utilized in situ small-angle X-ray scattering (in situ SAXS) and coherent X-ray scattering (CXS) to analyze the dynamics and gelation mechanism of three types of chitosan-based self-healing hydrogels with different dynamic interactions. In situ SAXS revealed the nucleation and growth mechanism for the gelling process, which has not been reported in a system of self-healing hydrogels. The critical nucleation radius (CNR) with different interactions could further influence the gelation rate and self-healing ability. Moreover, the continuous time-resolved CXS profile unveiled the dynamic behavior of different self-healing hydrogels in mesoscale, supported by rheological experiments. Information linking the rheological properties and structural changes could be useful in designing self-healing hydrogels for biomedical applications.

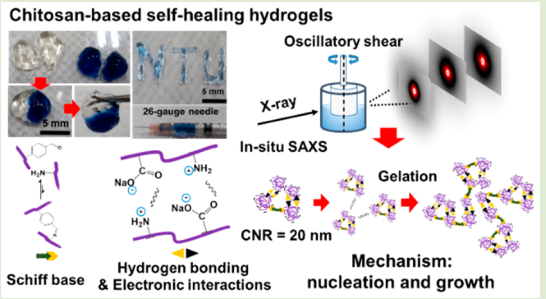

Hydrogels are a three-dimensional network of polymers cross-linked through conventional covalent bonds, dynamic covalent bonds, or physical interaction, resembling the extracellular matrix of the human body. In recent years, hydrogels have been studied extensively, including self-healing, nanocomposite, 3-D printing, thermoresponsive, and double network hydrogels.[1−5] With tunable mechanical properties, biocompatibility, injectability, and water retention capacities through chemical synthesis, hydrogels are potential biomaterials for biomedical applications. Self-healing hydrogels are defined as hydrogels that can heal the damage caused by an external force and recover mechanical properties automatically. Self-healing hydrogels contain reversible dynamic bonds, such as hydrogen bonds, Schiff base, Diels−Alder reaction, boronate ester bonds, host−guest chemistry, hydrophobic interactions, ionic interactions, and metal−ligand coordination.[6−14]

Naturally derived polymers such as chitosan, alginate, and hyaluronic acid are proper candidates for the preparation of self-healing hydrogels.[15−17] Chitosan (CS) is derived from chitin with good biocompatibility, low cytotoxicity, appropriate biodegradability, and convenient functionalization and has popular biomedical applications in wound dressing and drug delivery.[18,19] Polyethylene glycol with both ends functionalized by 4-formylbenzoic acid (DF-PEG) is a common cross-linker to prepare chitosan-based self-healing hydrogels.[20] Various water-soluble chitosan derivatives with low cytotoxicity and suitable solubility in the physiological environment have been widely used to prepare the self-healing hydrogels in recent research.[21−26] Although chitosan-based self-healing hydrogels are well developed, the structural changes in nanoscale during the gelation process are not investigated so far.

Small angle X-ray scattering (SAXS) is a powerful tool for structural analysis of materials, for example, measuring the ordered structure of the system, geometrical shapes, and hierarchical structures at the nanoscale. By calculating the correlation length of the fragile structure, the coherence decay of the logarithmic correlation function within the fractal structure could be studied.[27] SAXS and rheological experiments were employed to determine the fractal dimension values of various hydrogels, where a higher fractal dimension was found to promote cell proliferation and affect the differentiation fate of stem cells.[28] SAXS was also used to show the structure collapse of a pH-response self-healing hydrogel, where Fe^{III} interacted with modified polyallylamine as the pH varied to cause different cross-linking and fluctuation in scattering intensity.[29] Another self-healing hydrogel with guest−host chemistry was analyzed by SAXS, where the scattering intensity of the hydrogels was higher than that of solution, inferring cross-linked networks.[30] Although SAXS analysis was employed in the two systems of self-healable hydrogels, the in situ SAXS examination of the sol−gel

Received: August 28, 2019
Accepted: October 9, 2019
Published: October 11, 2019

Downloaded via SYNCHROTRON RADIATION RESEARCH on January 9, 2020 at 04:45:00 (UTC).
See https://pubs.acs.org/sharingguidelines for options on how to legitimately share published articles.

© 2019 American Chemical Society

DOI: 10.1021/acsmacrolett.9b00683
ACS Macro Lett. 2019, 8, 1449−1455

transition and the nucleation mechanism have seldom been reported in the literature.

The synchrotron X-ray source with improved intensity and coherence allows the studies of high-resolution SAXS and second order of dynamic structural changes. Here, in this study, we report the structural analysis for chitosan-based self-healing hydrogels by coherent X-ray scattering and SAXS, combined with an in situ rheometer. The nanoscale structure and gelling process of self-healing hydrogels are examined through the time-resolved operation of in situ SAXS and CXS, and real-time information regarding how hydrogels transform from sol to gel can be obtained. We demonstrate that the viscoelasticity and self-healing ability of hydrogels can be modulated by changing the dynamic interactions in self-healing hydrogels and the main chain of chitosan derivatives.

Various biocompatible, self-healing hydrogels were prepared from different chitosan-derived polymers cross-linked by DF-PEG, as illustrated in Figure 1A. The Schiff base, between the

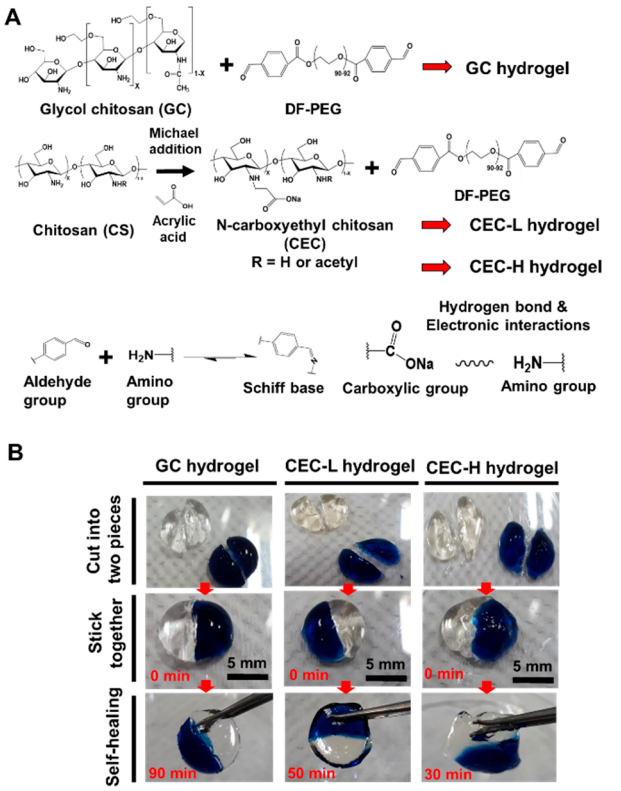

Figure 1. Schematic representation of self-healing hydrogels examined in this study and macroscopic self-healing observation. (A) Glycol chitosan forms self-healing hydrogel via dynamic covalent bonding with the cross-linker DF-PEG. *N*-Carboxyethyl chitosan (CEC), having different degrees of substitution, also forms self-healing hydrogel when cross-linked with DF-PEG via Schiff base and hydrogen bond interactions. (B) Samples were cut into two pieces and stuck back next to each other. All the hydrogels later recovered their shape and could be picked up by tweezers without breaking the integrated gel from the boundary of the two pieces.

amino groups of chitosan and the aldehyde groups of DF-PEG, endowed the hydrogel with the self-healing ability. The carboxylic group and amino group of CEC could form the intermolecular hydrogen bonds, which also provided hydrogels with the self-healing ability.[31] Hydrogels formed after mixing the chitosan (3 wt %) and cross-linker (2 wt %) solutions at equal volumes in room temperature. Water-soluble glycol chitosan (GC, 410 kDa, degree of deacetylation 78.2%, Wako) was used as received. CEC was synthesized from chitosan (CS, 170 kDa, degree of deacetylation 97%, Kiotec) based on the literature.[32] By adjusting the reaction temperature (50 or 70 °C), CEC with a lower degree (25.4%) of substitution (CEC-L) and with a higher degree (65.4%) of substitution (CEC-H) was obtained. The degree of substitution was measured using the ^{1}H NMR spectroscopy, as shown in Figure S1. The functionality of DF-PEG, defined by the ^{1}H NMR spectrum in Figure S2, was 81.3%, representing that 81.3% of the synthesized DF-PEG was difunctional.

The physicochemical properties of chitosan derivatives were performed by Fourier-transform infrared spectroscopy (FT-IR) and X-ray diffraction (XRD). The functional groups of CEC were examined by the FT-IR spectra and compared to those of CS, as shown in Figure S3A. The amino and hydroxyl groups showed the broad peak at 3453 cm^{-1} (−NH stretching, −OH stretching), amide bond at 1646 cm^{-1}, (−NH_2 bond) at 1594 cm^{-1}. Moreover, the new peak at 1579 cm^{-1} in the spectrum of CEC-L represented the asymmetrical vibration of the carboxyl group (−COO stretching). On the other hand, the new peak at 1561 cm^{-1} in the spectrum of CEC-H also represented the contribution from the carboxyl group. The results supported that the Michael addition of chitosan and acrylic acid occurred. The XRD patterns of chitosan derivative powders are demonstrated in Figure S3B. The chitosans have two typical peaks at 2θ = 10.2 and 20.0 corresponding to the crystal forms 1 and 2, according to the literature.[33] GC and CS had the broad band at 2θ = 13.5 and the peak at 2θ = 20.0, showing the crystallinity of CS was higher than that of GC. Meanwhile, CEC-L and CEC-H had only one broad band at 2θ = 13.5, suggesting that the N-carboxyethylation reaction changed the intermolecular interactions in chitosan.

The macroscopic self-healing observation of the hydrogels is shown in Figure 1B. The cut semidisc pieces of the CEC-H hydrogel quickly turned into an integrated circular piece of hydrogel and recovered the mechanical stability after 30 min. The diffusion of the blue dye could be observed from the junction of the two semidiscs in the CEC-H hydrogel. Meanwhile, CEC-L and GC hydrogels resumed one piece after 50 and 90 min, respectively. All the healed hydrogels could be picked up and shaken by tweezers without breaking the integrated gel from the boundary of the two semidisc pieces. For practical use, the injectability of the self-healing hydrogels is shown in Figure S4. the CEC-H hydrogel after gelation could still pass through a smaller gauge needle (26G) compared to the other hydrogels.

The rheological properties of CEC-L and CEC-H self-healing hydrogels were examined by a rheometer (Rheometric HR-2, TA Instruments) with the cone−plate geometry at 37 °C and the results are displayed in Figure 2. Table 1 shows the amino/aldehyde group molar ratio, storage modulus (G'), and gelation time of the self-healing hydrogel. For comparison, the rheological properties of the GC hydrogel are shown in Figure S5. To examine the sol−gel transition of CEC hydrogels, the shear strain dependent G' and loss modulus (G'') at 1 Hz are shown in Figure 2A,B. The CEC-L hydrogel was damaged at the shear strain 200%, where the G' decreased from 1 kPa to 150 Pa. Meanwhile, the CEC-H hydrogel was damaged at the strain 50%, where the G' was reduced from 3 to 0.2 Pa. A shear strain larger than the critical strain was then used for the damage process in testing the self-healing properties. The

DOI: 10.1021/acsmacrolett.9b00683
ACS Macro Lett. 2019, 8, 1449−1455

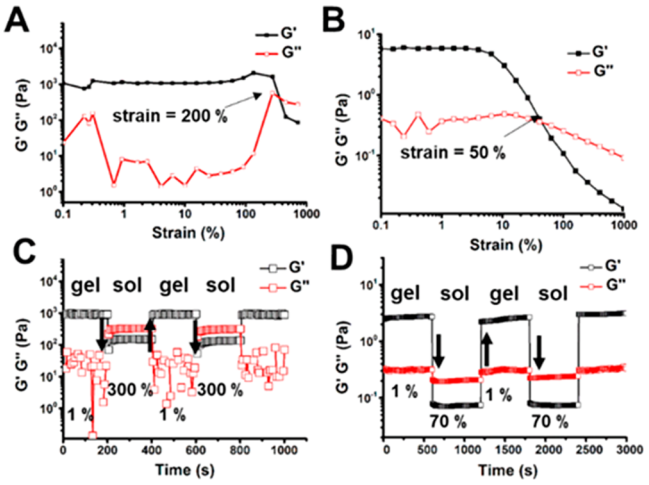

Figure 2. Rheological properties of CEC hydrogels at 37 °C. (A, B) The strain-dependent G' and G'' of CEC-L and CEC-H hydrogels by strain sweep experiments at 1 Hz. (C, D) The self-healing behavior of CEC-L and CEC-H hydrogels by the damage-healing cycles. The oscillatory strains for the damage process were (C) 300% and (D) 70% for CEC-L and CEC-H hydrogels, respectively. Healing was operated under 1% oscillatory strain at 1 Hz for both groups.

Table 1. Amine/Aldehyde Molar Ratio, Storage Modulus (G'), and Gelation Time of Different Self-Healing hydrogels[a]

self-healing hydrogel	NH_2/CHO	modulus (G')	gelation time
GC	10:1	1.5 kPa	~3 min
CEC-L	6.7:1	1 kPa	~5 min
CEC-H	3.3:1	3~10 Pa	~10 min

[a]All samples were prepared with the same final weight concentration of chitosan (1.5 wt %) and cross-linker DF-PEG (1 wt %) at room temperature.

continuous step strain change from 300% to 1% was used for damage-healing cycles of CEC-L hydrogel in Figure 2C. The continuous step strain change from 70% to 1% was used for the damage-healing cycles of CEC-H hydrogel in Figure 2D. The G' of each hydrogel was immediately recovered to its original value at the lower strain (1%).

To analyze the gelling process of self-healing hydrogels, in situ SAXS combined with a rheometer (Physica MCR-501, Anton Paar) using a double-cylinder rotator was conducted at the beamline 23A of National Synchrotron Radiation Research Center (Hsinchu, Taiwan). Results from in situ SAXS experiments of the self-healing hydrogels are shown in Figure 3. The storage modulus (G') and loss modulus (G'') were examined at the constant frequency of 1 Hz and oscillatory strain of 1%. Each SAXS frame of the exposure time (200 s) was simultaneously collected. The modulus (G') of GC hydrogel reached 1 kPa at the time of 4000 s in Figure 3A. Meanwhile, the G' of CEC-L hydrogel reached 100 Pa at the time of 6000 s in Figure 3C, and the G' of CEC-H hydrogel reached 10 Pa rather quickly at the time of 1500 s in Figure 3E. The SAXS profiles of the hydrogels are shown in Figure 3B, D, and F. The nanoscale structure did not change with time and may be explained by the nucleation and growth mechanism. The nucleation and growth mechanism was used to explain the formation of gold nanoparticles, silica nanoparticles, polymer crystallization, and so on.[34−37] The schematics in Figure 4E shows the hypothetical model of nucleation and growth for the

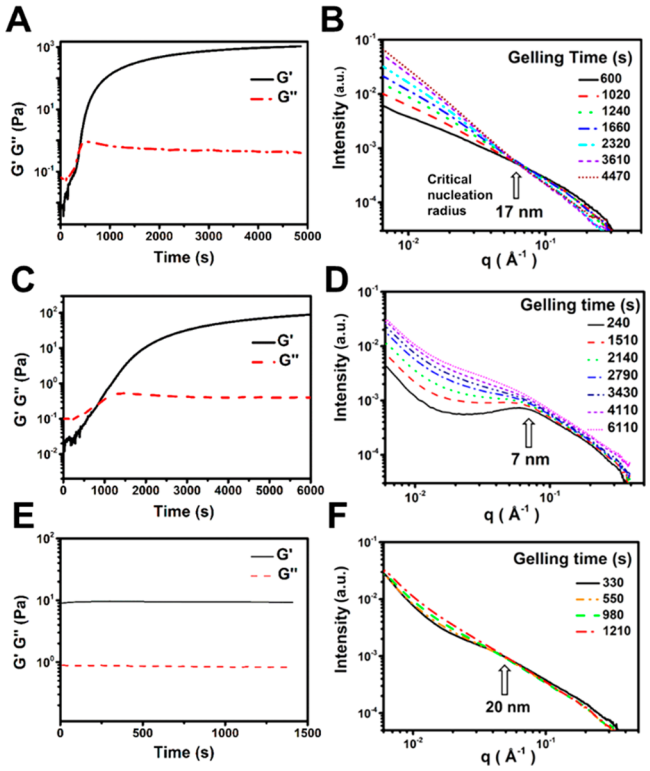

Figure 3. In situ rheological properties (time sweep) and SAXS profiles for different self-healing hydrogels: (A, B) GC hydrogel, (C, D) CEC-L hydrogel, and (E, F) CEC-H hydrogel.

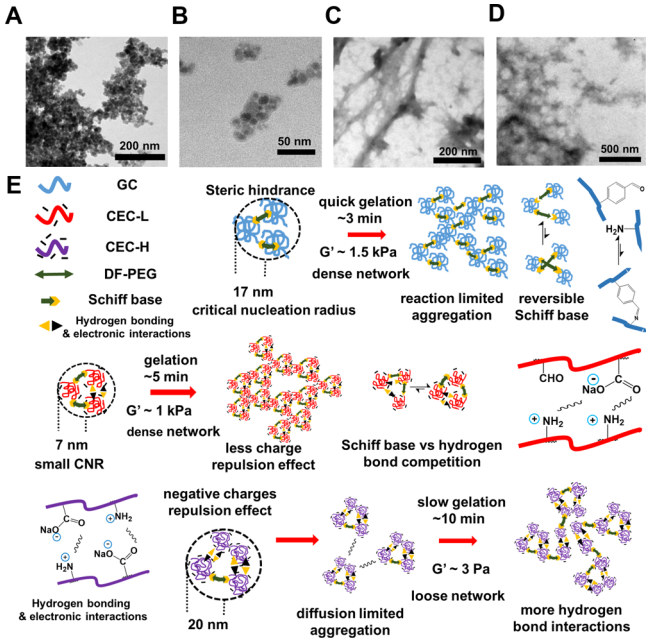

Figure 4. Gelation through nucleation. TEM images of (A, B) CEC-H hydrogel, (C) GC hydrogel, and (D) CEC-L hydrogel showing the aggregation of nuclei structure and the network of hydrogel. (E) Schematics for the gelation of various self-healing hydrogels through the hypothetical nucleation and growth mechanism.

self-healing hydrogels and dynamic interactions. Transmission electron microscopy (TEM) images, as shown in Figure 4A−D, revealed the aggregation of the nuclei structure and the network of hydrogel, supporting the mechanism of nucleation

DOI: 10.1021/acsmacrolett.9b00683
ACS Macro Lett. 2019, 8, 1449−1455

and growth. The critical nucleation radius of GC hydrogel was 17 nm, which was calculated by the q values of the scattering vector in the plot. The critical nucleation radius of CEC-L hydrogel was 7 nm, that is, smaller than that of GC. CEC-H hydrogel had a nucleation radius of 20 nm, that is, slightly larger than that of GC. By the Guinier analysis, the gyration radius (R_g) of various hydrogels was also obtained, as listed in Figure S6.

Results from the coherent X-ray scattering and rheological time-sweep test are presented in Figure 5. The dynamics of

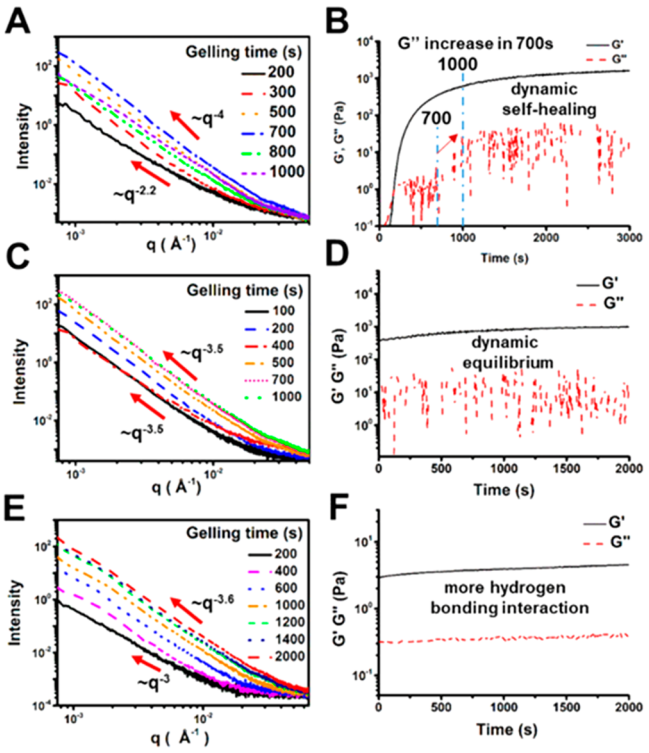

Figure 5. Sol−gel transition of different self-healing hydrogels probed by the coherent X-ray scattering (CXS) at the constant exposure time of 25 s. A total of 40 images were continually processed during the gelling period of 1000 s for (A) GC hydrogel, (B) CEC-L hydrogel, and (C) CEC-H hydrogel. The storage (G') and loss (G'') moduli as a function of gelling time by dynamic time sweep experiment of the (B) GC hydrogel, (D) CEC-L hydrogel, and (F) CEC-H hydrogel performed at the constant frequency = 1 Hz and strain γ = 1% during a period of 3000 s, showing the oscillation of G'' values.

self-healing hydrogels was revealed as the increasing intensity with gelling time. The storage modulus (G') and loss modulus (G'') were measured against time (3000 s) at the frequency of 1 Hz, and hydrogels underwent the sol−gel transition during the time sweep test. The curve of GC hydrogel (Figure 5A) reached the intensity maximum at the time of 700 s, decreased in 800 s, and slightly increased in 1000 s, indicating the dynamic behavior of self-healing hydrogels. The G'' of GC hydrogel as shown in Figure 5B supported the dynamic behavior of self-healing hydrogels. The fluctuation and a sudden increase in 1000 s of G'' indicated that the cleavage and regeneration of the imine bonds occurred and then the network of hydrogel reached the dynamic equilibrium. CEC-L hydrogel had G'' fluctuation (Figure 5D), suggesting the dynamic equilibrium of Schiff base and less hydrogen bonding interaction in comparison to CEC-H hydrogel. The CXS curve of CEC-L hydrogel (Figure 5C) went down in 400 s and then increased again in 500 s, causing the intensity fluctuation. Meanwhile, the G'' of the CEC-H hydrogel (Figure 5F) remained relatively flat, which implied that hydrogen bonding, electronic interactions, and Schiff base in the CEC-H hydrogel may compete with each other in forming the gel network. The CXS data (Figure 5E) showed the slow dynamics, where the curve reached the intensity maximum at the time of 2000 s. The fractal dimension of hydrogels was calculated based on the power law and the slopes of the curves. The fractal dimension of the GC hydrogel increased from 2.2 to 4, indicating that GC hydrogel shifted from mass fractal (2.2) to surface fractal (4) as the gelling time increased. The fractal value changes may indicate the different types of the cluster aggregation.

With the aid of FT-IR and XRD, the physicochemical characteristics of each chitosan derivative were obtained. The peak shift shown in the FT-IR spectra represented the newly generated carboxyl group compared to CS. The XRD data of CEC suggested that the introduction of carboxylic group in chitosan may interfere with the hydrogen bonding of amino group in chitosan. In addition, the mechanical properties of CEC-H self-healing hydrogel with more hydrogen bonding were quite similar to those of the human tissue that also possessed self-healing behavior.[38] Moreover, TEM images revealed that GC hydrogel had a dense network, while CEC-H had a loose network. These results suggested that the network of the hydrogel may be related to the structure arrangement

In this study, CEC hydrogels exhibited excellent self-healing ability in the continuous damage-healing cycles and in the visual observation. The introduction of zwitterionic CEC for preparing self-healing hydrogels may not only tune the storage modulus but also regulate the self-healing ability. Moreover, we observed that neural stem cells could survive well in either type of CEC self-healing hydrogels (Figures S7), suggesting that CEC-based self-healing hydrogels were biocompatible and may be suitable for biomedical applications.

The gel-forming process of hydrogels during the time sweep rheological experiment was further investigated by the in situ SAXS. The nucleation and growth mechanism suggested by the data of in situ SAXS with the increasing gelling time has not been seen in previous literature for the system of the self-healing hydrogels. The nucleation and growth mechanism was conventionally used to explain the crystal growth of metallic materials and was more recently found to be applicable in describing the gelation of the physical hydrogels and the formation of the nanoparticles in solution.[39−41] The hypothetical scheme is shown in Figure 4. Each hydrogel was generated from clusters of a critical nucleation radius (CNR), and the nuclei aggregated to form the 3-D network of the hydrogel. TEM images supported the nuclei structure for the network of hydrogel (Figure 4A−D). The larger CNR may be explained based on the repulsion of negative charge, steric effect, and molecular weight of chitosan. Moreover, the CNR of the hydrogel may affect the gelation time. GC hydrogel with a larger CNR value showed a shorter gelation time, probably because clusters of large nuclei may quickly aggregate. However, CEC hydrogels had nuclei with a more abundant negative charge, which may slow down the gelling rate due to cluster repulsion and steric hindrance. Meanwhile, the hydrogen bonds from the carboxyl group may enhance the self-healing ability of the hydrogel.[42] The electronic interactions in CEC hydrogels brought about by the more

DOI: 10.1021/acsmacrolett.9b00683
ACS Macro Lett. 2019, 8, 1449−1455

abundant negative charges could promote the self-healing ability.[43]

Coherent X-ray scattering (CXS) at the beamline 25A of Taiwan Photon Source (TPS) with an excellent light source (photon flux = 10^{12} photons/sec) and an applicable q range (0.0006 to 0.7 $Å^{-1}$) could provide the nanoscale information of soft materials. The time-dependent fluctuations in the scattering pattern could yield insight into the structural dynamics of the hydrogels.[44,45] Results revealed that the scattering intensity of all hydrogels increased with gelling time, where the intensity converged in the high q region (q > 0.01). The intensity tendency of CXS was similar to that observed by the in situ SAXS, further supporting the nucleation and growth mechanism. However, the curve of the GC hydrogel in Figure 5A shows that the CXS intensity first increased and then decreased, supporting the G'' fluctuation of dynamic self-healing behavior in Figure 5B. The uncoupling and recoupling of the imine linkages occur dynamically in the self-healing hydrogel.[46] The introduction of hydrogen bonds and electronic interactions in CEC may alter the dynamics of self-healing hydrogels. In the CEC-L hydrogel, the CXS intensity variation and G'' fluctuation suggested the presence of more Schiff base and less hydrogen bond interaction in the hydrogel. In the CEC-H hydrogel, G'' values were relatively flat without fluctuation compared to those observed in GC and CEC-L hydrogels. Meanwhile, the intensity of the CXS data increased with gelling time without variation, suggesting an influence by hydrogen bonding and electronic interactions. The different extents of G'' fluctuation in time-sweep rheological curves (Figures 3 and 5) were caused by the usage of different rotators in rheometry. Moreover, the fractal dimension of hydrogels could reflect the aggregation mechanism of the gel. The growth of gel network is affected by the reaction-limited or diffusion-limited aggregation.[47] The fractal dimension of 2.2 of the GC hydrogel suggested that the initial gelation of GC hydrogel may be affected by the Schiff reaction-limited aggregation of nuclei. Meanwhile, the surface fractal of the CEC-H hydrogel varied from 3.0 to 3.6, suggesting that the diffusion-limited aggregation of CEC-H hydrogel may rely on the formation of hydrogen bonds and diffusion of nuclei with negative charges. Based on the above results, the time-dependent CXS experiment could reveal the dynamic bond formation of the hydrogel, providing more details on the nanostructure change associated with the reversible dynamics of the hydrogel during gelation.

In summary, we prepared the self-healing hydrogels based on zwitterionic chitosan derivatives (CEC) with different substitution and glycol chitosan (GC) to investigate their gelation mechanism and structural dynamics. The properties of various chitosan-based self-healing hydrogels were investigated with regard to their different CNR. We demonstrated that CEC hydrogels exhibited unique rheological properties, internal morphology, and self-healing behavior. In particular, we employed the approaches of in situ SAXS and CXS to establish the nucleation mechanism of self-healing hydrogels and the structural dynamics during the sol−gel transition. The nucleation and growth mechanism has rarely been reported in a self-healing hydrogel system. By correlating the gelling process and dynamic bonds of hydrogels, it is expected that future applications can be applied to the preparation of other self-healing hydrogels with different CNRs. Hydrogels with more abundant negative charges in the main chain may facilitate the self-healing process, while hydrogels with more Schiff base could enhance the gelling rate. The in-depth knowledge and understanding of the gelation mechanism and self-healing dynamics will assist in the design and optimization of self-healing hydrogels for future basic research and applications.

■ ASSOCIATED CONTENT

Supporting Information

The Supporting Information is available free of charge on the ACS Publications website at DOI: 10.1021/acsmacrolett.9b00683.

Details of the materials and methods, NMR spectra of chitosan, CEC-L, and CEC-H, NMR spectrum of DF-PEG, FT-IR spectra and XRD patterns of chitosan derivatives, needle injectability of the self-healing hydrogels, rheological profiles of GC hydrogel by strain sweep test and damaging−healing cycles, Guinier analysis of hydrogels, and cell viability of neural stem cells (PDF)

■ AUTHOR INFORMATION

Corresponding Author

*Phone: +886-2-3366-5313. Fax: +886-2-3366-5237. E-mail: shhsu@ntu.edu.tw.

ORCID

Wei-Tsung Chuang: 0000-0002-9000-2194

Shan-hui Hsu: 0000-0003-3399-055X

Notes

The authors declare no competing financial interest.

■ ACKNOWLEDGMENTS

This work was supported by the Ministry of Science and Technology (MOST 108- 2221-E-002-082-MY3), Taiwan, and partially supported by National Taiwan University (Grant No. 108L891101). We also thank National Synchrotron Radiation Research Center (2019-1-209) and the staffs of TLS beamline 23A and TPS beamline 25A, in particular, Dr. U-Ser Jeng and Dr. Yu-Shan Huang for providing the resources and technical support.

■ REFERENCES

(1) Pan, C.; Liu, L.; Chen, Q.; Zhang, Q.; Guo, G. Tough, stretchable, compressive novel polymer/graphene oxide nanocomposite hydrogels with excellent self-healing performance. *ACS Appl. Mater. Interfaces* **2017**, *9* (43), 38052−38061.

(2) Taylor, D. L.; in het Panhuis, M. Self-healing hydrogels. *Adv. Mater.* **2016**, *28* (41), 9060−9093.

(3) Ouyang, L.; Highley, C. B.; Rodell, C. B.; Sun, W.; Burdick, J. A. 3D printing of shear-thinning hyaluronic acid hydrogels with secondary cross-linking. *ACS Biomater. Sci. Eng.* **2016**, *2* (10), 1743−1751.

(4) Chen, Q.; Zhu, L.; Zhao, C.; Wang, Q.; Zheng, J. A robust, one-pot synthesis of highly mechanical and recoverable double network hydrogels using thermoreversible sol-gel polysaccharide. *Adv. Mater.* **2013**, *25* (30), 4171−4176.

(5) Yan, Y.; Li, M.; Yang, D.; Wang, Q.; Liang, F.; Qu, X.; Qiu, D.; Yang, Z. Construction of injectable double-network hydrogels for cell delivery. *Biomacromolecules* **2017**, *18* (7), 2128−2138.

(6) Zhang, G.; Chen, Y.; Deng, Y.; Ngai, T.; Wang, C. Dynamic supramolecular hydrogels: regulating hydrogel properties through self-complementary quadruple hydrogen bonds and thermo-switch. *ACS Macro Lett.* **2017**, *6* (7), 641−646.

DOI: 10.1021/acsmacrolett.9b00683
ACS Macro Lett. 2019, 8, 1449−1455

(7) Wei, Z.; Lewis, D. M.; Xu, Y.; Gerecht, S. Dual Cross-Linked Biofunctional and Self-Healing Networks to Generate User-Defined Modular Gradient Hydrogel Constructs. *Adv. Healthcare Mater.* **2017**, *6* (16), 1700523.
(8) Yu, F.; Cao, X.; Du, J.; Wang, G.; Chen, X. Multifunctional hydrogel with good structure integrity, self-healing, and tissue-adhesive property formed by combining Diels−Alder click reaction and acylhydrazone bond. *ACS Appl. Mater. Interfaces* **2015**, *7* (43), 24023−24031.
(9) He, L.; Szopinski, D.; Wu, Y.; Luinstra, G. A.; Theato, P. Toward self-healing hydrogels using one-pot thiol−ene click and borax-diol chemistry. *ACS Macro Lett.* **2015**, *4* (7), 673−678.
(10) Rodell, C. B.; Kaminski, A. L.; Burdick, J. A. Rational design of network properties in guest−host assembled and shear-thinning hyaluronic acid hydrogels. *Biomacromolecules* **2013**, *14* (11), 4125−4134.
(11) Sun, Y.; Wollenberg, A. L.; O'Shea, T. M.; Cui, Y.; Zhou, Z. H.; Sofroniew, M. V.; Deming, T. J. Conformation-directed formation of self-healing diblock copolypeptide hydrogels via polyion complexation. *J. Am. Chem. Soc.* **2017**, *139* (42), 15114−15121.
(12) Cuthbert, T. J.; Jadischke, J. J.; de Bruyn, J. R.; Ragogna, P. J.; Gillies, E. R. Self-healing polyphosphonium ionic networks. *Macromolecules* **2017**, *50* (14), 5253−5260.
(13) Azevedo, S.; Costa, A. M.; Andersen, A.; Choi, I. S.; Birkedal, H.; Mano, J. F. Bioinspired Ultratough Hydrogel with Fast Recovery, Self-Healing, Injectability and Cytocompatibility. *Adv. Mater.* **2017**, *29* (28), 1700759.
(14) Wei, Z.; Yang, J. H.; Zhou, J.; Xu, F.; Zrínyi, M.; Dussault, P. H.; Osada, Y.; Chen, Y. M. Self-healing gels based on constitutional dynamic chemistry and their potential applications. *Chem. Soc. Rev.* **2014**, *43* (23), 8114−8131.
(15) Maity, S.; Datta, A.; Lahiri, S.; Ganguly, J. A dynamic chitosan-based self-healing hydrogel with tunable morphology and its application as an isolating agent. *RSC Adv.* **2016**, *6* (84), 81060−81068.
(16) Liu, S.; Kang, M.; Li, K.; Yao, F.; Oderinde, O.; Fu, G.; Xu, L. Polysaccharide-templated preparation of mechanically-tough, conductive and self-healing hydrogels. *Chem. Eng. J.* **2018**, *334*, 2222−2230.
(17) Loebel, C.; Rodell, C. B.; Chen, M. H.; Burdick, J. A. Shear-thinning and self-healing hydrogels as injectable therapeutics and for 3D-printing. *Nat. Protoc.* **2017**, *12* (8), 1521.
(18) Ravi Kumar, M. N.V A review of chitin and chitosan applications. *React. Funct. Polym.* **2000**, *46* (1), 1−27.
(19) Bhattarai, N.; Gunn, J.; Zhang, M. Chitosan-based hydrogels for controlled, localized drug delivery. *Adv. Drug Delivery Rev.* **2010**, *62* (1), 83−99.
(20) Zhang, Y.; Tao, L.; Li, S.; Wei, Y. Synthesis of multiresponsive and dynamic chitosan-based hydrogels for controlled release of bioactive molecules. *Biomacromolecules* **2011**, *12* (8), 2894−2901.
(21) Hamedi, H.; Moradi, S.; Hudson, S. M.; Tonelli, A. E. Chitosan based hydrogels and their applications for drug delivery in wound dressings: A review. *Carbohydr. Polym.* **2018**, *199*, 445−460.
(22) Tripodo, G.; Trapani, A.; Rosato, A.; Di Franco, C.; Tamma, R.; Trapani, G.; Ribatti, D.; Mandracchia, D. Hydrogels for biomedical applications from glycol chitosan and PEG diglycidyl ether exhibit pro-angiogenic and antibacterial activity. *Carbohydr. Polym.* **2018**, *198*, 124−130.
(23) Fan, M.; Ma, Y.; Tan, H.; Jia, Y.; Zou, S.; Guo, S.; Zhao, M.; Huang, H.; Ling, Z.; Chen, Y.; Hu, X. Covalent and injectable chitosan-chondroitin sulfate hydrogels embedded with chitosan microspheres for drug delivery and tissue engineering. *Mater. Sci. Eng., C* **2017**, *71*, 67−74.
(24) Yang, B.; Zhang, Y.; Zhang, X.; Tao, L.; Li, S.; Wei, Y. Facilely prepared inexpensive and biocompatible self-healing hydrogel: a new injectable cell therapy carrier. *Polym. Chem.* **2012**, *3* (12), 3235−3238.
(25) Qu, J.; Zhao, X.; Ma, P. X.; Guo, B. pH-responsive self-healing injectable hydrogel based on N-carboxyethyl chitosan for hepatocellular carcinoma therapy. *Acta Biomater.* **2017**, *58*, 168−180.
(26) Wei, Z.; Yang, J. H.; Liu, Z. Q.; Xu, F.; Zhou, J. X.; Zrínyi, M.; Osada, Y.; Chen, Y. M. Novel biocompatible polysaccharide-based self-healing hydrogel. *Adv. Funct. Mater.* **2015**, *25* (9), 1352−1359.
(27) Chen, S.-H.; Teixeira, J. Structure and fractal dimension of protein-detergent complexes. *Phys. Rev. Lett.* **1986**, *57* (20), 2583.
(28) Hung, K.-C.; Jeng, U.-S.; Hsu, S.-h. Fractal structure of hydrogels modulates stem cell behavior. *ACS Macro Lett.* **2015**, *4* (9), 1056−1061.
(29) Krogsgaard, M.; Behrens, M. A.; Pedersen, J. S.; Birkedal, H. Self-healing mussel-inspired multi-pH-responsive hydrogels. *Biomacromolecules* **2013**, *14* (2), 297−301.
(30) Himmelein, S.; Lewe, V.; Stuart, M. C.; Ravoo, B. J. A carbohydrate-based hydrogel containing vesicles as responsive non-covalent cross-linkers. *Chem. Sci.* **2014**, *5* (3), 1054−1058.
(31) Xue, S.; Wu, Y.; Guo, M.; Liu, D.; Zhang, T.; Lei, W. Fabrication of Poly (acrylic acid)/Boron Nitride Composite Hydrogels with Excellent Mechanical Properties and Rapid Self-Healing Through Hierarchically Physical Interactions. *Nanoscale Res. Lett.* **2018**, *13* (1), 393.
(32) Yang, S.; Dong, Q.; Yang, H.; Liu, X.; Gu, S.; Zhou, Y.; Xu, W. N-carboxyethyl chitosan fibers prepared as potential use in tissue engineering. *Int. J. Biol. Macromol.* **2016**, *82*, 1018−1022.
(33) Samuels, R. J. Solid state characterization of the structure of chitosan films. *J. Polym. Sci., Polym. Phys. Ed.* **1981**, *19* (7), 1081−1105.
(34) Polte, J. r.; Ahner, T. T.; Delissen, F.; Sokolov, S.; Emmerling, F.; Thünemann, A. F.; Kraehnert, R. Mechanism of gold nanoparticle formation in the classical citrate synthesis method derived from coupled in situ XANES and SAXS evaluation. *J. Am. Chem. Soc.* **2010**, *132* (4), 1296−1301.
(35) Fouilloux, S.; Désert, A.; Taché, O.; Spalla, O.; Daillant, J.; Thill, A. SAXS exploration of the synthesis of ultra monodisperse silica nanoparticles and quantitative nucleation growth modeling. *J. Colloid Interface Sci.* **2010**, *346* (1), 79−86.
(36) Chen, J.; Schneider, K.; Kretzschmar, B.; Heinrich, G. Nucleation and growth behavior of β-nucleated iPP during shear induced crystallization investigated by in-situ synchrotron WAXS and SAXS. *Polymer* **2014**, *55* (21), 5477−5487.
(37) Su, C.-H.; Wu, W.-R.; Chen, C.-Y.; Su, C.-J.; Chuang, W.-T.; Liao, K.-F.; Chen, S.-H.; Su, A.-C.; Jeng, U.-S. Nanograin nucleation at the growth front in melt crystallization of syndiotactic polystyrene. *Polymer* **2016**, *105*, 414−421.
(38) Ding, D.; Guerette, P. A.; Fu, J.; Zhang, L.; Irvine, S. A.; Miserez, A. From Soft Self-Healing Gels to Stiff Films in Suckerin-Based Materials Through Modulation of Crosslink Density and β-Sheet Content. *Adv. Mater.* **2015**, *27* (26), 3953−3961.
(39) Thanh, N. T.; Maclean, N.; Mahiddine, S. Mechanisms of nucleation and growth of nanoparticles in solution. *Chem. Rev.* **2014**, *114* (15), 7610−7630.
(40) Crompton, K.; Prankerd, R.; Paganin, D.; Scott, T.; Horne, M.; Finkelstein, D.; Gross, K.; Forsythe, J. Morphology and gelation of thermosensitive chitosan hydrogels. *Biophys. Chem.* **2005**, *117* (1), 47−53.
(41) Wang, Y.; Li, B.; Zhou, Y.; Jia, D. In situ mineralization of magnetite nanoparticles in chitosan hydrogel. *Nanoscale Res. Lett.* **2009**, *4* (9), 1041.
(42) Xue, S.; Wu, Y.; Guo, M.; Liu, D.; Zhang, T.; Lei, W. Fabrication of Poly (acrylic acid)/Boron Nitride Composite Hydrogels with Excellent Mechanical Properties and Rapid Self-Healing Through Hierarchically Physical Interactions. *Nanoscale Res. Lett.* **2018**, *13* (1), 393.
(43) Cheng, K.-C.; Huang, C.-F.; Wei, Y.; Hsu, S.-h. Novel chitosan−cellulose nanofiber self-healing hydrogels to correlate self-healing properties of hydrogels with neural regeneration effects. *NPG Asia Mater.* **2019**, *11* (1), 25.
(44) Czakkel, O.; Nagy, B.; Geissler, E.; László, K. Effect of molybdenum on the structure formation of resorcinol−formaldehyde hydrogel studied by coherent x-ray scattering. *J. Chem. Phys.* **2012**, *136* (23), 234907.

DOI: 10.1021/acsmacrolett.9b00683
ACS Macro Lett. 2019, 8, 1449−1455

(45) van der Veen, F.; Pfeiffer, F. Coherent X-ray scattering. *J. Phys.: Condens. Matter* **2004**, *16* (28), 5003.
(46) Tseng, T. C.; Tao, L.; Hsieh, F. Y.; Wei, Y.; Chiu, I. M.; Hsu, S. h. An injectable, self-healing hydrogel to repair the central nervous system. *Adv. Mater.* **2015**, *27* (23), 3518−3524.
(47) Liao, W.; Zhang, Y.; Guan, Y.; Zhu, X. Fractal structures of the hydrogels formed in situ from poly (N-isopropylacrylamide) microgel dispersions. *Langmuir* **2012**, *28* (29), 10873−10880.

DOI: 10.1021/acsmacrolett.9b00683
ACS Macro Lett. 2019, 8, 1449−1455